OPTOELECTRONICS AND ADVANCED MATERIALS – RAPID COMMUNICATIONS Vol. 15, No. 11-12, November-December 2021, p. 528 - 537

Investigation of the effect of photonic crystal geometry on the absorption spectrum

M. SOLAIMANI[a], PARISA MAHMOUDI[b,*]
[a]*Department of Physics, Qom University of Technology, Qom, Iran*
[b]*Department of Electrical and Computer Engineering, Qom University of Technology, Qom, Iran*

In this paper, we investigate the different forms of photonic crystal geometries and calculate the absorption diagrams and we try to obtain the maximum absorption. The effects of size and the number of photonic crystal holes and their shapes have been studied. The proposed structures can have absorption coefficients of higher than 98%. The dielectric function of the gallium arsenide layer is calculated by Maxwell Garnet model.

(Received June 12, 2021; accepted November 24, 2021)

Keywords: Two dimensions' photonic crystals, Size effect, Different shapes of photonic crystal holes, Maxwell-Garnet Model, Absorption spectrum

1. Introduction

Optical devices are the basic elements of electronics and telecommunications technology, where information is transmitted at high speed [1]. More than two decades of acoustic and mechanical wave control by periodic patterning of materials has been considered and periodic pattern dielectric media or photonic crystals lead to a series of scientific and technical breakthroughs in the way of light [2]. One of the reasons that has made us interested in research on photon crystals is that photonic crystals in all scientific fields, including electronics, communications, antennas, medical industries, laser devices in nature, etc.

The creation and introduction of photonic crystals has become important with the conversion of light into an electronic chip [3]. Photonic crystals are defined in one, two and three dimensions so that one dimensional photonic crystals are very strong in light control and have been used for more than 70 years for a laser cavity in light structures. Light control of two and three dimensional photonic crystals is easier. The research on photonic crystals was started by E. Yablonovitch and S. John in theory and is still considered by optical devices [3,4]. An example of a one-dimensional photonic crystal is an array of scattered polystyrene suspended particles in water. The three dimensional photonic crystal resembles a jewel because of Bragg's scattering under white light. Two, three dimensional examples of photonic crystals are currently being studied more [5] and two-dimensional photonic crystals are a good choices for optical processing devices [6]. Photonic crystals are alternating structures with an array of dielectric layers where their refractive index is repeated periodically. Photonic crystals have attracted much attention for their ability to control the electromagnetic wave using the photonic crystal band gap concept [7-9]. Photonic crystals have attracted a lot of theoretical and experimental attentions because they have applications in fields ranging from basic physics to communication systems [10]. One of the new solutions for photonic crystal is to create adjustable optical delay for a variety of applications of photonic systems, including for telecommunication systems, antennas and optical communication networks [11-13]. In photonic crystals, where several light spectra are absorbed by photons, the absorption spectrum is a good way to achieve the optimal amount of optical spectra [14]. Photonic crystals are used in the design of integrated optical circuits such as waveguides, filters, resonators, and lasers, and because of their multi-micrometer dimensions, they provide many applications [15-19]. One of the reasons for the stability of using cryptocurrencies in optical devices is also to control the diffusion of light inside the structure [3]. However, one of the most important applications of photonic crystal is in microwave signal processing [20].

The photonic crystal cavities block the light and the amount of light emitted from the small space of these cavities. The main characteristic of photonic crystals is that they have a photon band gap for photons [1, 21-22], which is similar to the electronic band structure for semiconducting electrons [23]. The transmission of electromagnetic waves in a specific frequency range called the band gap is forbidden [3-4]. One of the important features of the photonic crystals is the surface Plasmon, which is caused by the oscillations of the conduction band charge electrons in a metal or the landing electromagnetic wave of a surface-polarity wave. The electromagnetic field of the surface Plasmon wave propagates on the metal surface and fluctuates perpendicular to the surface in both directions (positive, negative) [2]. As presented in 2005, a quantum dot –based optical structure using photonic crystals has been used to increase the detector quantum efficiency by up to 93%, while this parameter for a similar structure without a photonic crystal was about is 7%. In 2006 they provided a more complete report of this

structure, and by placing ab absorption layer on the cavities, showed that the light flow was increased more than once.

Photonic crystals have several solution methods, including Maxwell's equations, the blob function theory, and the surface wave method. Also, another method called Brilliance areas in the reverse network is one of the other methods of calculating the gap in photonic crystals. The finite difference time domain (FDTD) method, can also solve the Maxwell's equations. Such types of calculations can also be done using the famous transfer matrix method [33-35]. By studying the quantum dot-based optical devices, we came to the conclusion that the quantum dots absorb a small percentage of the light due to their doting, and therefore, the use of metallic crystallography is one of the techniques used to increase the absorption. Also, one of the latest developments of photonic crystals is the low-power thermal switching, which uses photons with a fano structure and a p-i-n connection [31].

The purpose of changing the geometry of the photonic crystal on the absorption spectrum is to find its effects, for example, high cross-sectional or triangular or pentagonal geometries that have sharp corners and cause the input light to be wasted on the absorption spectrum. Also we want to know the extent of the geometry changes effects on the amount of light trapped.

2. Numerical model

Light is a kind of electromagnetic wave that is applied to the structure. In the slab of the structure, because the polarization in the radiation plane is along the vibration of the electric field, it is TE wave. Landing light with TE polarization and rectangular input port boundary conditions is applied throughout the structure, making the output port smaller than the input to minimize the output light loss and absorbing more light in the structure. The dielectric function is calculated in the dipole approximation. The polarization in an atomic system with a wave function $\Psi(\mathrm{r},\mathrm{t})$ is given [26]:

$$\rho_a(t) = -<e(t)>\int \Psi^*(r,t)(-er)\Psi(r,t)dr \qquad (1)$$

where e is the electron charge. Equation (1) can be written by Fourier transform in the frequency domain as

$$\rho_a(t) = \frac{\mathrm{E}}{\hbar}\sum_l e^2 \left|<\varphi_0|r|\varphi_1>\right|^2 \left(\frac{1}{\omega_l - \omega - i\gamma_l} + \frac{1}{\omega_l + \omega + i\gamma_l}\right) \qquad (2)$$

where E is the magnitude of the electric field φ_o and φ_1 are the atomic wave functions in the excited and ground states, respectively, and γ_l is the amplitude parameter and ω_l is the transition frequency. In an environment containing a set of oscillators with density N, the polarization density is defined as follows [26]:

$$\mathrm{P}(\omega) = \mathrm{N}\rho_a(\omega) = \varepsilon_0\chi(\omega)\mathrm{E}(\omega) \qquad (3)$$

and the definition of a dimensionless quantity called oscillator strength is required in the relationship of the effective dielectric function **[**26**]**:

$$f_l = \frac{2m_0\omega_l}{\hbar}<\varphi_0|\rho|\varphi_1>^2 = \frac{2}{2m_0\omega_l}<\varphi_0|\rho|\varphi_1>^2 \qquad (4)$$

Using high permeability equations, an environment is defined as follows,

$$\varepsilon(\omega) = 1 - \sum_l \frac{\mathrm{N}e^2 f_l / m_0\varepsilon_0}{\omega^2 - \omega_l^2 + i\,2\omega\gamma_l} \qquad (5)$$

Considering the effect of electron transitions on a background constant ε_b, the above relation can be rewritten as [26].

$$\varepsilon_{QD}(\omega) = \varepsilon_b + \frac{2}{V_{QD}}\left[f_c(E_c) - f_v(E_v)\right]\frac{e^2 f / m_{0\varepsilon_0}}{\omega^2 - \omega_0^2 + i\,2\omega\gamma} \qquad (6)$$

where f is the oscillator strength in the transition of inter-band and f_c and f_v are distribution functions of the carriers in the conductivity and the valence band, respectively. γ and ω are the transition frequencies and the broadening parameter, respectively. Effective dielectric function of InAs/GaAs QD layer ($\varepsilon_{eff}(\omega)$) is calculated through modified Maxwell-Garnett (MMG) model [28]:

$$\frac{\varepsilon_{eff}(\omega) - \varepsilon_b}{\varepsilon_{eff}(\omega) + 2\varepsilon_b} = f_{QD}\int_0^\infty dx\,(x/x_0)^3 P(x) + \frac{\varepsilon_{QD}(\omega,x) - \varepsilon_b}{\varepsilon_{QD}(\omega,x) + 2\varepsilon_b} \qquad (7)$$

where ε_b is bulk dielectric constant, f_{QD} is QD fraction considered as 0.2 here, x is QD radius and x_0 is average of QDs radius and P(x) quantum dot size distribution function. $\varepsilon_{QD}(\omega)$ in Eq. (7) is single QD dielectric function.

$$P(x) = \frac{1}{x\sqrt{2\pi}Log(\sigma)} \times \exp\left(-\left((Log(x/x_0)/(\sqrt{2}Log(\sigma))\right)^2\right) \qquad (8)$$

It is also the standard deviation provided by [29]

$$Log(\sigma) = \left[\sum_i N_i (Log(x_i) - Log(x_0))^2 \Big/ \sum_i N_i\right]^{0.5} \qquad (9)$$

The optical properties of composite films embedded in other layers can be obtained from models such as Maxwell-Garnett or Bruggeman theory effective medium approximations. However, the Maxwell-Garnett model allows the explicit consideration of size dispersion of the holes in the photonic crystal [32]. Therefore, we used it.

The absorption spectrum obtained using the algorithms used in the powerful software of Comsol Multiphysics.

3. Results and discussion

Proposed structures are shown in the following Structures are simulated in two-dimensional space in COMSOL multiphysics optical software [30]. We study the geometric shapes of the photonic crystal nanoparticles and their numbers on the slabs of the optical structure. The photonic crystal geometry has holes containing air and has circular geometries, and each circle is further elongated, and the holes inside the slab are 8 μm long and 10 μm wide.

In the next steps, each time the circle was stretched to b = 0.30um and the number of horizontal and vertical rows is 6 × 6 as before. We reduced the b value by 0.25, 0.20, 0.15 and 0.10 μm, which makes the circle more elongated and the absorption spectrum is 1 to 8 μm in the wavelength range below.

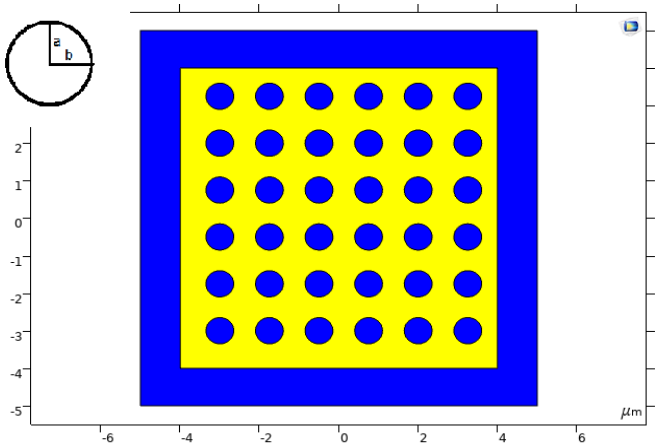

Fig. 1. Geometry of circular photonic crystal. Blue color show air holes. Yellow color, layer of gallium arsenide slab extracted from Maxwell's equations. The cavity radius is 0.35 μm and grid constant is 1.25 μm (color online)

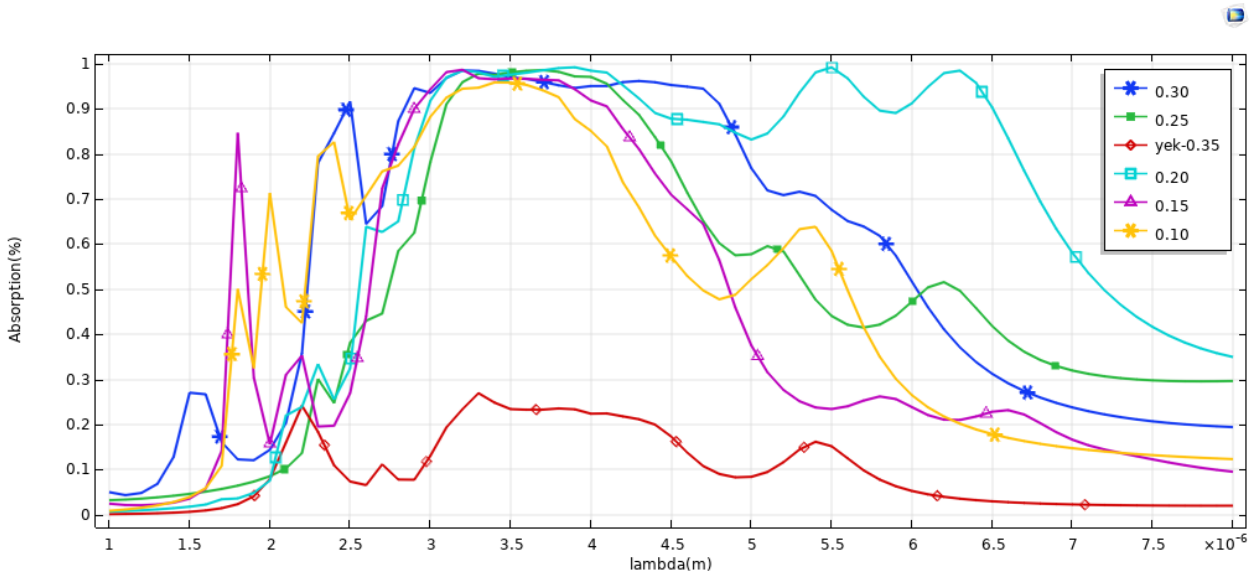

Fig. 2. Comparison of the absorption spectrum of the circular holes, the one-0.35 word, the circle with a radius of 0.35 μm and the value a, b is the same (color online)

Result of comparison of absorption spectra in circular shapes:

In this graph the absorption spectra of most of the investigated radii have optimum absorption and absorption in the range of 3 to 4 μm, blue diagram has high absorption in wide range 3. It is up to 6.5 μm. So it is suitable for high absorption applications over a wide frequency range. If the hole is circular, i.e. the value of a, b = 0.35 um, the absorption is almost low at all frequency bands that is suitable for low absorption applications. However, with the help of 'a' to 'b' ratio, the absorption can be adjusted at any interval between zero and one.

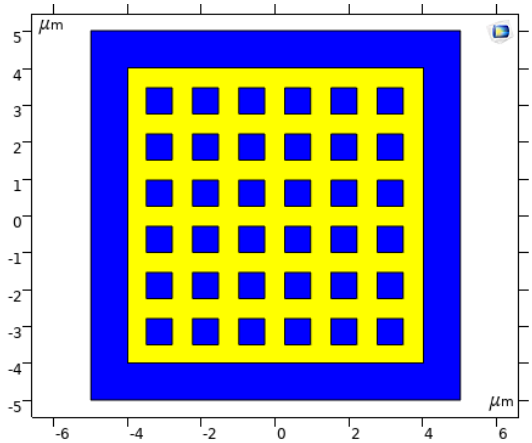

Fig. 3. Photonic crystal geometry with square-shaped cavities that are their length are 0.7 μm (color online)

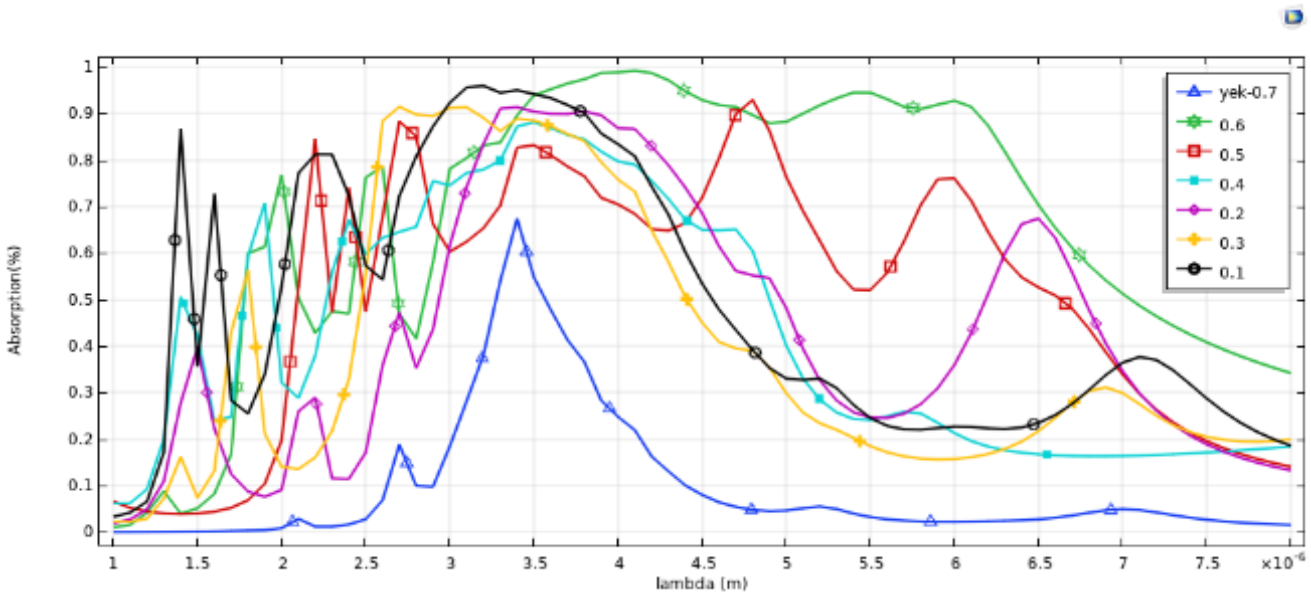

Fig. 4. Comparison of the absorption spectrum of the square photonic crystal geometry. 0.7 means a square with a length and width of 0.7 μm and the values of a, b are the same (color online)

Absorption spectrum results in different square shapes:

In this graph, the absorption spectra of the green diagram have a high absorbance over the wavelength range of 3.5 to 6.5 μm and are therefore are suitable for high absorption applications over the long wavelength range. A rectangle with a wavelength range of 3 to 4 μm has the maximum absorption value. A square geometry having a length and width of 0.7 μm has the lowest absorption at all wavelengths and is therefore suitable for low absorption applications. By adjusting the length and width of the hole, the absorption value is calculated for the high absorption users.

At this stage, holes are the hexagons that are located inside the GaAs slab.

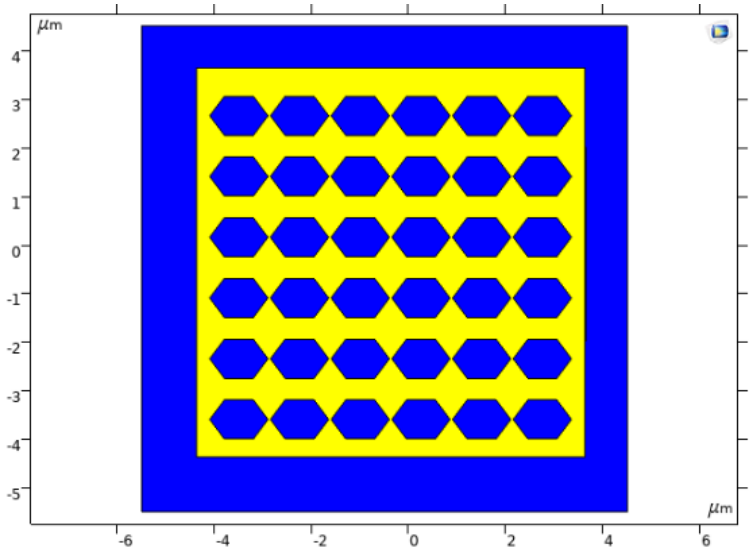

Fig. 5. Hexagonal photonic crystal geometry, having hexagonal coordinates of 0.4, 0.6, and 0.3 μm. the lattice constant of 1.25 μm and 6 × 6 are assumed (color online)

In the next step, we put just one hexagon in the middle of the slab with dimensions of 1.5, 3.5 and 1.5 μm. The next are the hexagons with coordinates of 0.3, 1.7 and 0.3 μm.

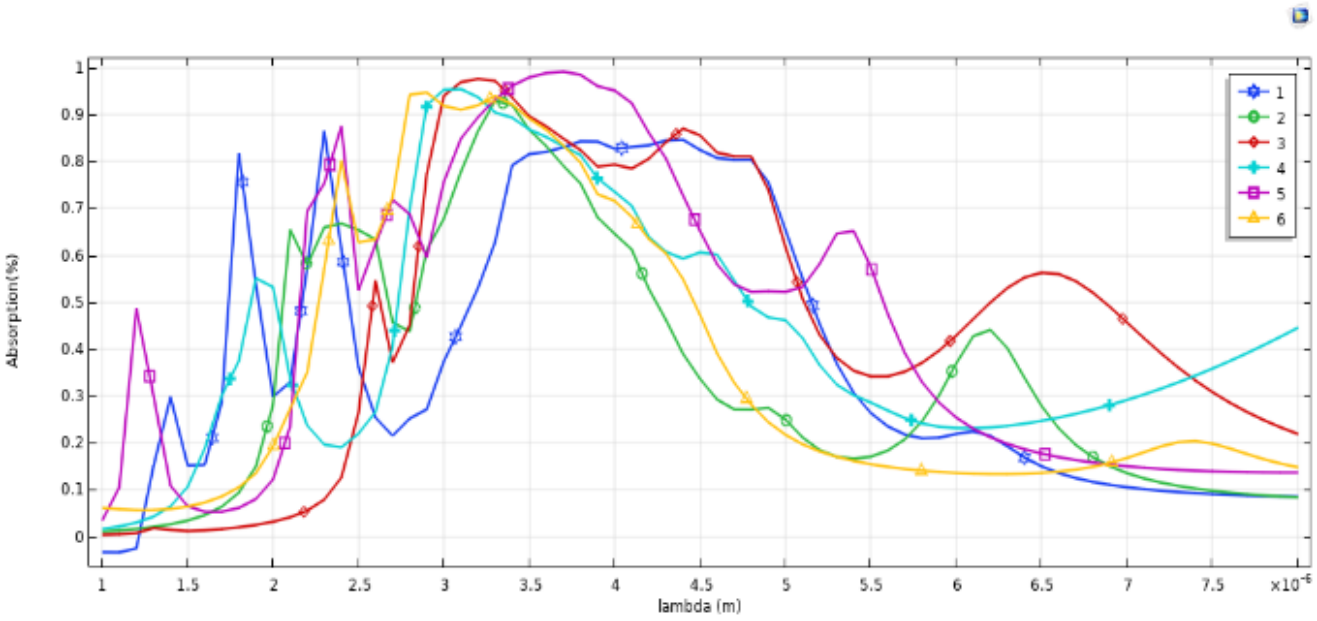

Fig. 6. Comparison of the absorption spectra of the hexagonal photonic crystal cavities Figs. 1 to 6 (color online)

Comparison of absorption spectra:

In the absorption spectrum graph of the hexagonal shapes in the wavelength range 2.8 μm to 4 μm, most of the modes have the maximum absorption value and the purple diagram has optimum absorption over wide wavelength range. The blue diagram at low wavelength range 6.5 to 8 μm has low absorption value which is suitable for low absorption applications.

Now, the photonic crystal cavities are pentagonal inside the slab at 0.5 μm and 0.6 μm at the bottom side, there are 6 rows and 6 columns with a lattice constant of 1.25 μm.

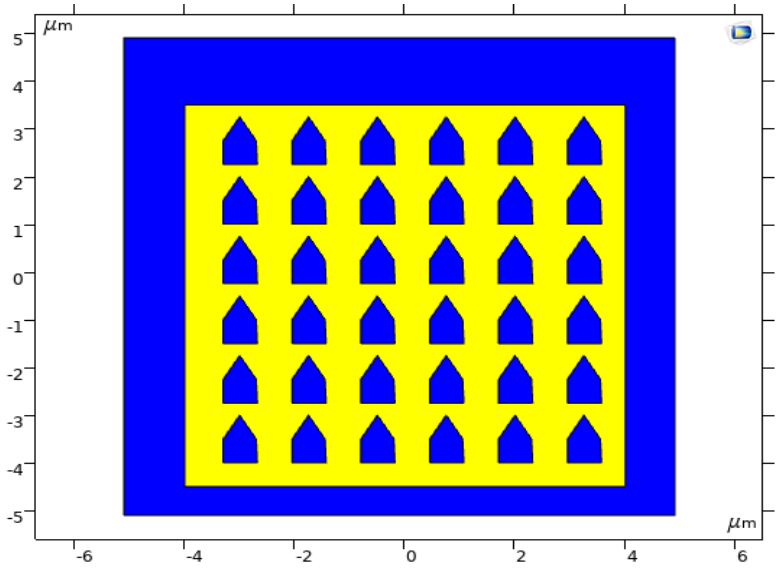

Fig. 7. Photonic crystal geometry of pentagonal cavities (color online)

In the next step, all the sides are 0.5 μm and the bottom side 0.4 μm, with 6 rows, 6 columns and 1.25 μm grid constants. Then, all the sides are 0.5 μm and the bottom side is 0.2 μm and there are 6 rows and 6 columns and a grid constant of 1.25 μm.

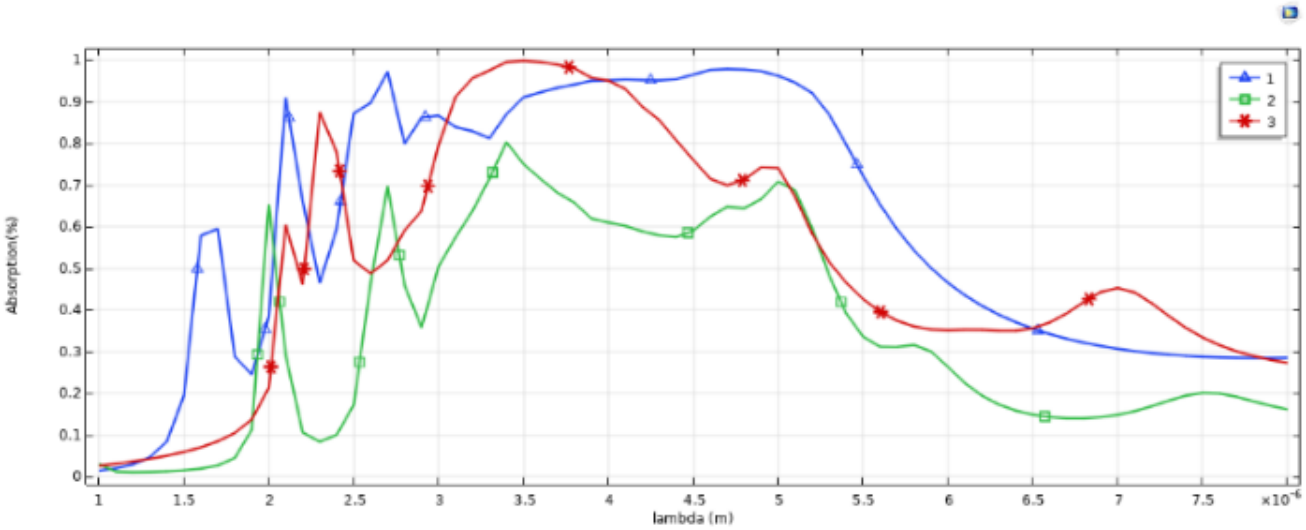

Fig. 8. Comparison of absorption spectra of pentagonal photonic crystal holes in steps 1 to 3 (color online)

Comparison of absorption spectra:

In pentagonal shapes, the green graph has the lowest absorption value in all the wavelength ranges and is suitable for low absorption applications. At the wavelength 3.3 μm, the red graph has an optimum absorption value of 1. This wavelength is 3.3 μm in the infrared spectrum range and is used for infrared detectors to achieve high absorption. The wavelength has maximum absorption and 98% absorption in the wavelength range 4.5 to 5 μm.

Here, we calculated the kagome geometry with different materials and absorption spectra.

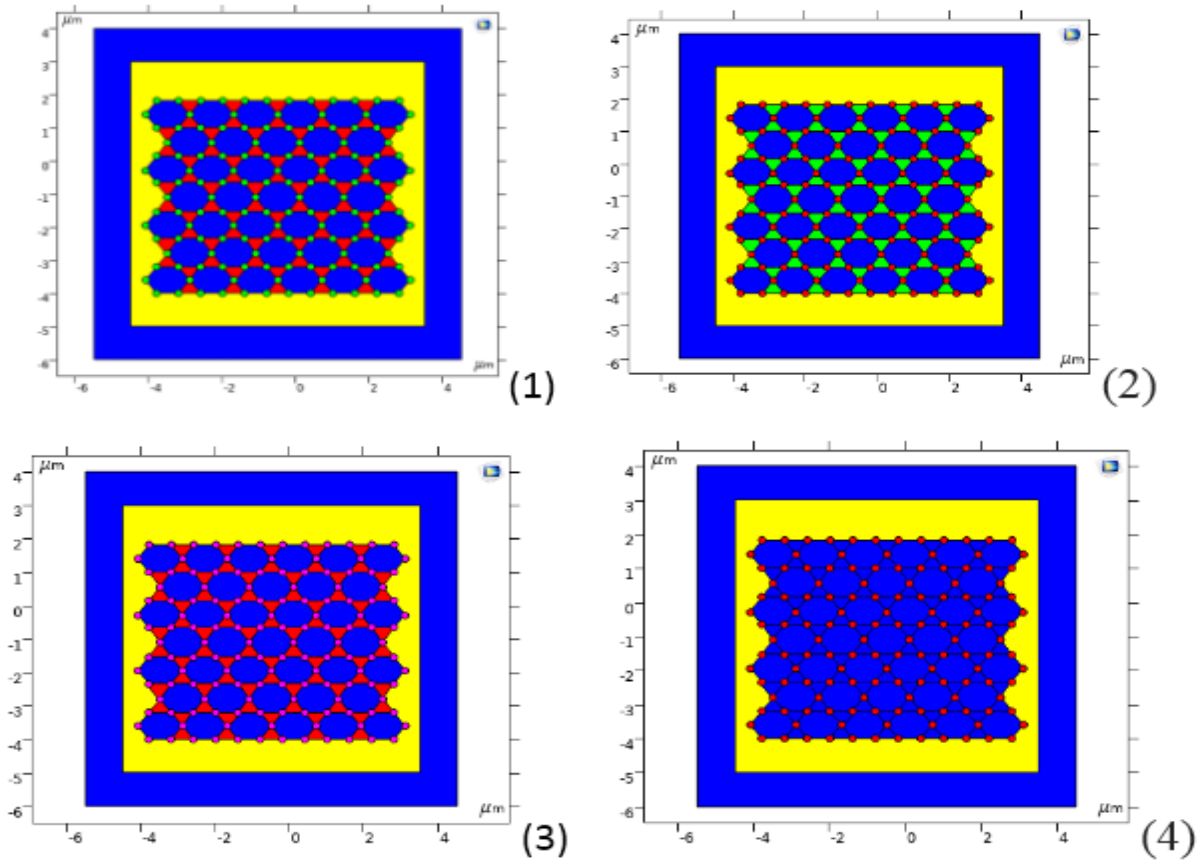

Fig. 9. Kagome geometry panels (1), (2), (3), and (4) (color online)

Panel (1) is the Kagome geometry of gallium arsenide, germanium and silicon materials. The blue colors are air and yellow are gallium arsenide. Also, green parts are germanium while the red is silicon.

Panel (2) is Kagome geometry of gallium arsenide, germanium and silicon materials. The blue is air and yellow is slabs of gallium arsenide. Germanium green and silicon are red.

Panel (3) is Kagome geometry of gallium arsenide, germanium and silicon materials. The blue is air and the yellow is layer of gallium arsenide. The red is silicon and pink is indium phosphate.

Panel (1) is Kagome geometry of gallium arsenide, germanium and silicon materials. The blue is the air and the yellow is the layer of gallium arsenide. The red is silicon.

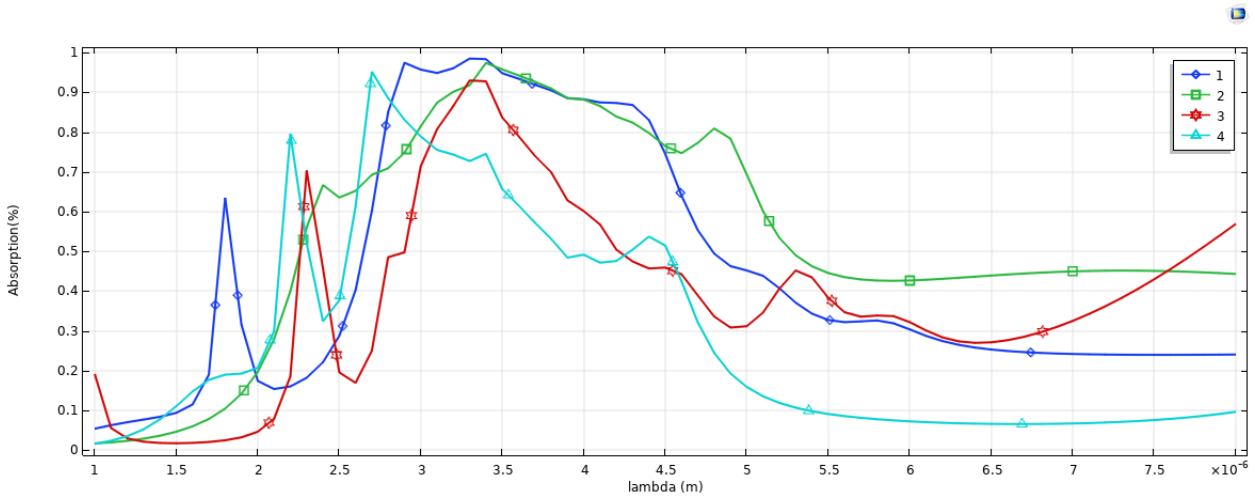

Fig. 10. Comparison of absorption spectrum of kagome geometry from steps 1 to 4 (color online)

Comparison of absorption spectra of kagome geometries with different materials:

From absorption diagram in the wavelength range of 2.8 μm to 3.3 μm, the blue diagram has an optimum absorption value of 99% and the green diagram has a wide absorption range of 2.4 μm to 8 μm with high absorption. The blue diagram over a wide range of 3 to 8 μm has low absorption and is suitable for low absorption applications. The absorption diagram shows that different materials in kagome geometry is highly adsorbed.

At this point, the photonic crystal cavities are crescent-shaped inside the slab (Figs. 11 and 13).

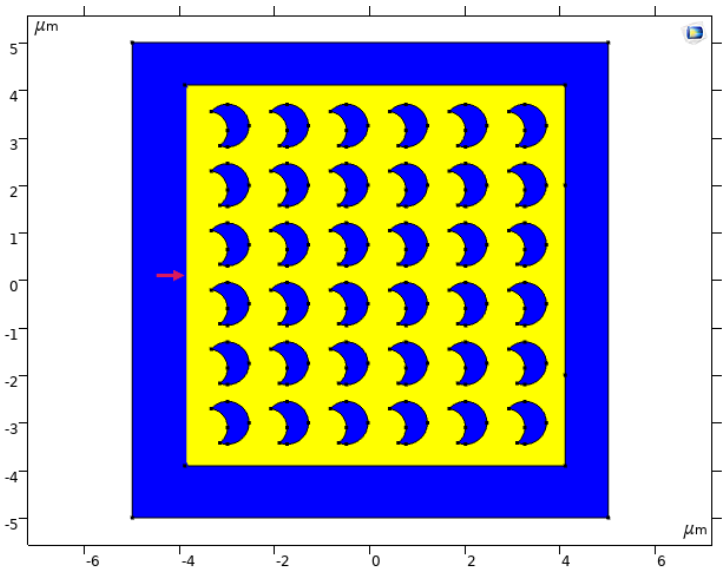

Fig. 11. Thick Crescent geometry (color online)

Crescent-shaped photonic crystal cavities composed from the air inside the gallium arsenide slab is studied. We reduced the crescent thickness each time and calculated their absorption diagram as Fig. 12.

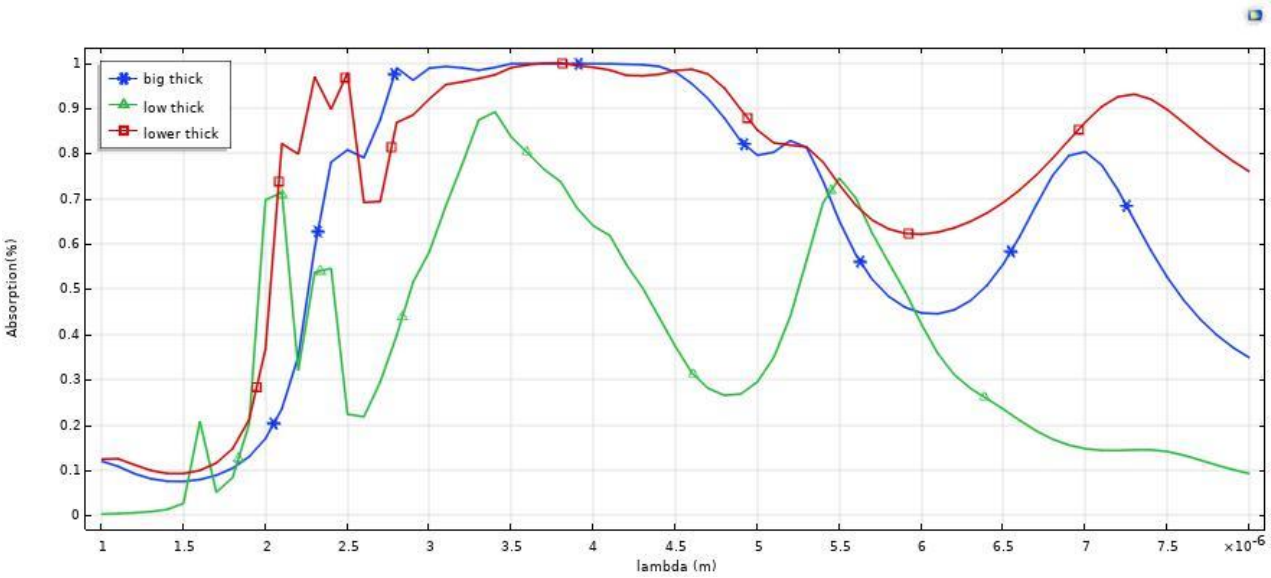

Fig. 12. Comparison of absorption spectrum of Crescent geometry (color online)

Comparison of absorption spectrum:

In Fig. 12, the absorption spectrum has three thicknesses with optimum absorption and the absorption is in the range 3 to 4.5 μm. The red graph has high absorption in the range 2 to 8 μm so are appropriate for high absorption applications over a wide range of frequencies. With the help of the thickness ratio, the absorption can be adjusted at any interval between zero and one. The structure shown in the next figure, have a high absorption.

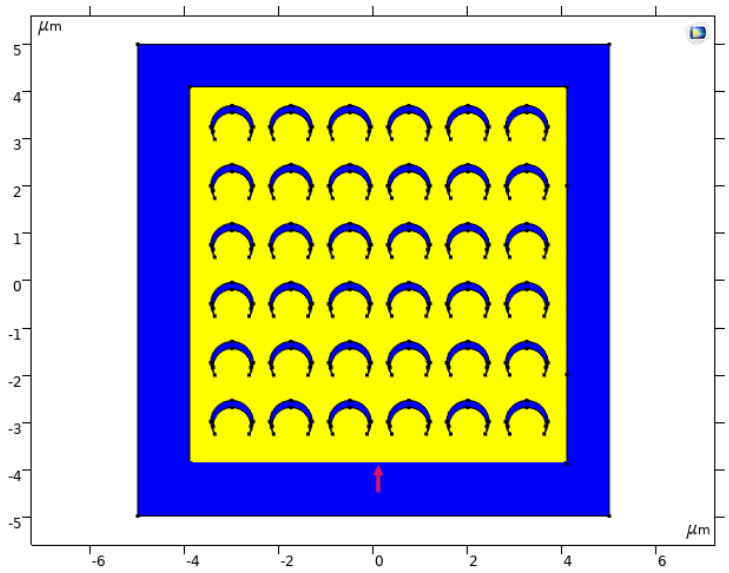

Fig. 13. Thin Crescent geometry (color online)

This time, we calculated absorption diagram of Fig. 13 is as in Fig. 14. The difference between the Figs. 11 and 13 is the position of the port. Then we compared the absorptions of three different crescents with different thicknesses as well as the effect of changing the port position.

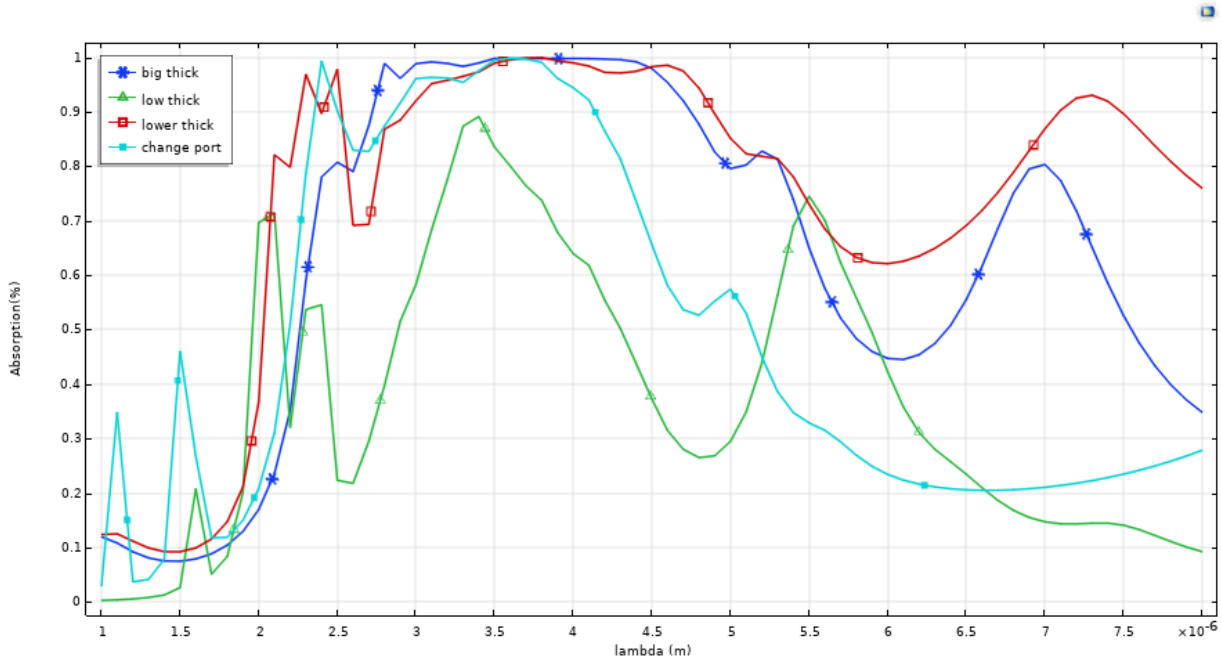

Fig. 14. Comparison of absorption spectrum of Crescent geometry (color online)

4. Conclusion

We proposed some complex optical structures with different forms of photonic crystals and the geometries with different materials. In fact, the photonic crystals are used to increase optical efficiency. Absorption is calculated using MMG model for effective dielectric function of QDs. The results showed that, there is an improvement in the absorption coefficient of the proposed structures up to 1. These structures can easily integrate with other optical devices.

References

[1] S. Kazuaki, Optical properties of photonic crystals, vol. **80**, eds. Springer Science & Business Media (2004).
[2] A. H. Safavi-Naeini, J. T. Hill, S. Meenehan, J. Chan, S. Gröblacher, O. Painter, Physical Review Letters **112**, 153603 (2014).
[3] E. Yablonovitch, Phys. Rev. Lett. 58, 2059 (1987).
[4] J. Sajeev, J. Wang, Phys. Rev. Lett. **64**, 2418 (1990).
[5] I. Kuon, K. Ohtaka, Photonic crystals: physics, fabrication and applications, vol. **94**, eds. Springer Science & Business Media (2004).
[6] K. Timo, A. Huttunen, P. Törmä, Journal of Applied Physics **96**, 4039 (2004).
[7] L. Cheng, X. Li, J. Sun, H. Zhong, Y. Tian, J. Wan, W. Lu, Y. Zheng, T. Yu, L. Huang, H. Yu, Physica B: Condensed Matter **405**, 4457 (2010).
[8] S. H. Kwon, H. Y. Ryu, G. H. Kim, Y. H. Lee, S. B. Kim, Applied Physics Letters **83**, 3870 (2003).
[9] Baba, Toshihiko, Naoyuki Fukaya, Jun Yonekura, Electronics Letters **35**, 654 (1999).
[10] K. J. Vahala, Nature (London) **424**, 839 (2003).
[11] Y. Okawachi, M. A. Foster, X. Chen, A. C. Turner-Foster, R. Salem, M. Lipson, C. Xu, A. L. Gaeta, Opt. Express **16**, 10349 (2008).
[12] W. Zheng, S. Fan, Physical Review E **68**, 066616 (2003).
[13] Y. Zhang, H. Wu, D. Zhu, S. Pan, Optics Express **22**, 3761 (2014).
[14] J. D. Joannopoulos, R. D. Meade, J. N. Winn, Photonic Crystals: Molding the Flow of Light, Princeton University Press, Princeton, NJ, 1995.
[15] M. D. B. Charlton, G. J. Parker, S. W. Roberts, Mater. Sci. Eng. B **49**, 155 (1997).
[16] T. Baba, IEEE J. Quantum Electron. **3**, 808 (1997).
[17] E. Istrate, E. H. Sargent, IEEE J. of Quantum Electronics **41**, 461 (2005).
[18] J. K. Poon, J. Scheuer, Y. Xu, A. Yariv, Journal of Optical Society of America B **21**, 1665 (2004).
[19] S. Lan, S. Nishikawa, H. Ishikawa, O. Wada, Journal of Applied Physics **90**, 4321 (2001).
[20] D. Marpaung, C. Roeloffzen, R. Heideman, A. Leinse, S. Sales, J. Capmany, Laser & Photon. Rev. **7**, 506 (2013).
[21] D. R. Smith, R. Dalichaouch, N. Kroll, S. Schultz, S. L. McCall, P. M. Platzman, Journal of Optical Society of America B **10**, 314 (1993).
[22] J. Liu, B. Shi, D. Zhao, X. Wang, Journal of Optics A: Pure and Applied Optics **4**, 636 (2002).
[23] M. Imada, S. Noda, A. Chutinan, T. Tokuda, M. Murata, G. Sasaki, Applied Physics Letters **75**, 316 (1999).
[24] E. A. R. Ortuno, J. Appl. Phys. **106**, 124313 (2000).

[25] T. W. Ebbesen, C. Genet, Nature **445**, 39 (2007).
[26] P. Holmström, L. Thylén, A. Bratkovsky, Journal of Applied Physics **107**, 064307 (2010).
[27] V. T. K. T. Posani, S. Annamalai, N. R. Weisse-Bernstein, S. Krishna, R. Perahia, O. Crisafulli, O. J. Painter, Appl. Phys. Letters **88**, 1 (2006).
[28] S. Krishna, K. T. Posani, V. Tripathi, S. Annamalai, IEEE LEOS Annual Meeting Conference Proceedings 909 (2005).
[29] R. K. Willardson, E. R. Weber, M. Sugawara, Academic Press (1999).
[30] https://www.comsol.com
[31] Q. Saudan, D. A. Bekele, A. Marchevsky, Y. Yu, L. K. Oxenløwe, K. Yvind, J. Mørk, M. Galili, 21st International Conference on Transparent Optical Networks (ICTON) IEEE (pp. 1-4), (2019).
[32] A. S. Keita, A. E. Naciri, Y. Battie, F. Delachat, M. Carrada, G. Ferblantier, A. Slaoui, Journal of Applied Physics **116**, 103520 (2014).
[33] B. F. Wan, Y. Xu, Z. W. Zhou, D. Zhang, H. F. Zhang, IEEE Sensors Journal **21**(3), 2846 (2020).
[34] S. Guo, C. Hu, H. Zhang, Journal of Optical Society of America B **37**(9), 2678 (2020).
[35] B. F. Wan, Z. W. Zhou, Y. Xu, H. F. Zhang, IEEE Sensors Journal **21**(1), 331 (2020).

*Corresponding author: Mahmoodi.parisa.9094@gmail.com